GCAGS JOURNAL
A Publication of the Gulf Coast Association of Geological Societies
www.gcags.org

BURIAL AND THERMAL HISTORY OF THE HAYNESVILLE SHALE: IMPLICATIONS FOR OVERPRESSURE, GAS GENERATION, AND NATURAL HYDROFRACTURE

Jeffrey A. Nunn

Department of Geology and Geophysics, Louisiana State University,
E235 Howe-Russell Complex, Baton Rouge, Louisiana 70803, U.S.A.

ABSTRACT

The Haynesville Shale is an organic rich sedimentary rock found in northwestern Louisiana, eastern Texas, and southwestern Arkansas. It was deposited during the Late Jurassic in a marine environment. Average thickness varies from 200 to 300 ft (60–90 m). The Haynesville Shale is typically found at depths of 10,000 ft (3 km) or more and is characterized by ultra low permeability. It is an area of active exploration and development for natural gas especially in northwestern Louisiana. Results from an earlier thermal-mechanical model suggest that Jurassic temperature gradients were more than twice the current regional value of 0.0135 to 0.02°F/ft (25 to 35°C/km). Thus, Jurassic age sediments have been close to their current temperatures for the last 100 m.y. Using subsurface data, a simple model of heat transport by advection and conduction and fluid flow by compaction was used to estimate temperature, maturation, and fluid pressure through time for the Haynesville Shale. High heat flow in the Early Cretaceous contributed to high temperature gradients and early maturation of hydrocarbons. Rapid sedimentation in the Early Cretaceous resulted in generation of significant overpressure within the Haynesville Shale. This overpressure cannot be maintained over geologic time because the unit is too thin and there was subsequent uplift and erosion. Hydrocarbon generation produced additional overpressure in the Late to mid-Cretaceous and the Late Paleogene. However, under most conditions, model overpressures do not exceed the fracture gradient.

INTRODUCTION

The Haynesville Shale unit within the Haynesville Formation is a target of active exploration and development for natural gas in northwestern Louisiana and eastern Texas (Fig. 1). It is an organic rich sedimentary rock deposited in a shallow marine environment during the Late Jurassic (Mancini et al., 2005, 2008). The Haynesville Shale is typically found at depths between 10,000 and 13,500 ft (3–4 km) and ranges in thickness from 200 to 300 ft (60–90 m). Porosity ranges from 3–14% and matrix permeability can be less than a nanodarcy (nd) (Wang and Hammes, 2010).

The Haynesville Formation overlies the Smackover Formation and is, in turn, buried by the Cotton Valley Group and a thick succession of Cretaceous sediment as well as some Tertiary sediment (Li, 2006; Mancini et al., 2006, 2008). The Haynesville Shale is thickest in the North Louisiana Salt Basin and thins over the Sabine Uplift along the Texas-Louisiana border (Fig. 1). The Tertiary section is also thickest in the North Louisiana Salt Basin and thins over the Sabine Uplift (Mancini et al., 2008). The Sabine Uplift was reactivated during the mid-Cretaceous generating erosion of as much as 2000 ft (600 m) (Granata, 1963; Halbouty and Halbouty, 1982; Jackson and Laubach, 1988; Li, 2006)

Nunn (1984) and Nunn et al. (1984) examined the subsidence and thermal history of the North Louisiana Salt Basin. Subsidence versus time from well data in northern Louisiana is consistent with rifting and extension of the lithosphere by a β factor of 1.25 to 2 depending on location (Nunn et al., 1984). The β factors are smaller over the Sabine Uplift and larger in the deepest parts of the North Louisiana Salt Basin. Rifting and extension of the lithosphere caused high heat flow which dissipated over time. Present-day geothermal gradients in northern Louisiana are 0.0135 to 0.02°F/ft (25 to 35°C/km) (D'Aquin and Nunn, 2010). However, Jurassic geothermal gradients estimated from a thermal-mechanical model of basin formation by rifting and extension of the lithosphere are more than 0.033°F/ft (60°C/km)

Manuscript received March 2, 2012; revised manuscript received May 18, 2012; manuscript accepted May 29, 2012.

GCAGS Journal, v. 1 (2012), p. 81–96.

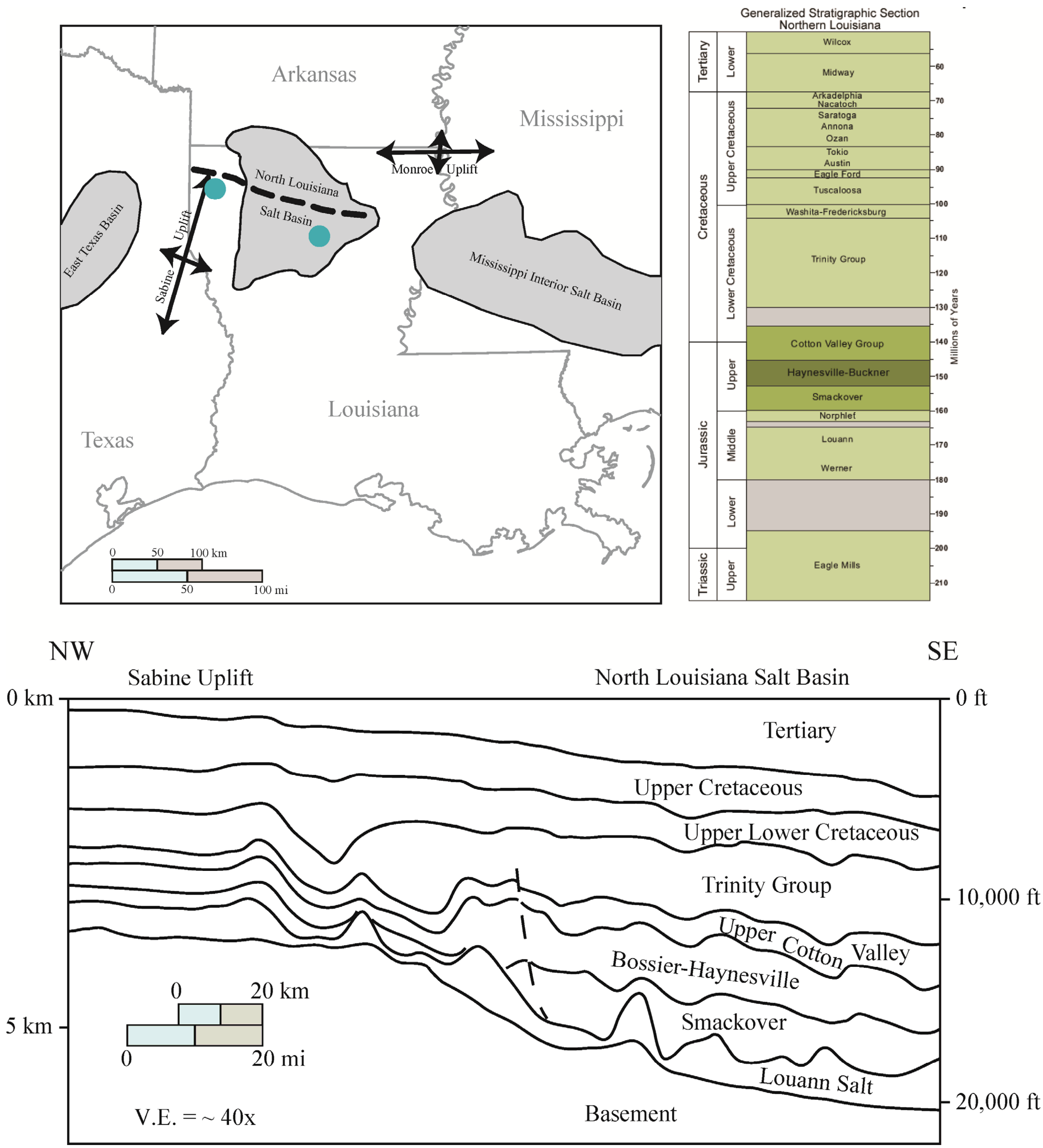

Figure 1. Top, left) Location map of study area including interior salt basins and related structural highs. Heavy, dashed line is location of cross-section shown below. Blue dots are well locations used in this study. Top, right) Stratigraphic column for northern Louisiana (modified after geology.com). Bottom) Northwest to southeast cross-section constructed from seismic and well data (modified after Mancini et al., 2008).

(Nunn, 1984). As a result, Jurassic sediments have been at essentially maximum burial temperatures since the mid-Cretaceous as thermal effects of deeper burial have been offset by a decline in basal heat flow.

A full core of the Haynesville Shale was displayed as part of a symposium at the Gulf Coast Association of Geological Societies meeting in Shreveport in 2009 (Berg et al., 2009). Visual inspection of the core revealed numerous fractures and many of these fractures had been resealed by cement indicating that they occurred by natural processes. Some of the cements are >0.25 in (>0.6 cm) thick which implies multiple phases of fracture and cementation. Natural hydrofractures in the Haynesville Shale also have been observed in core images and image logs (Buller and Dix, 2009; Fan et al., 2010). Natural hydrofracture could occur during burial if pore pressures exceed the fracture pressure or approximately 85% of lithostatic pressure (Hubbert and Willis, 1957).

Pore pressures in excess of hydrostatic pressure can be generated by disequilibrium compaction during rapid accumulation of low permeability sediments (Mello and Karner, 1996; Osborne and Swarbrick, 1997) as well as volume changes associated with the conversion of kerogen to oil and/or gas (Ungerer et al., 1983; Spencer, 1987; Hansom and Lee, 2005). In addition, if permeability is sufficiently low, then pore pressures may be maintained near maximum levels during uplift and erosion which could also push pore pressures near the fracture gradient as lithostatic pressure is reduced by erosion.

In this study a simple model of heat transport by advection and conduction and fluid flow by compaction was used to estimate temperature, maturation, and fluid pressure through time for the Haynesville Shale for two wells in north Louisiana (Fig. 1). Model results were used to determine the timing and capacity of fracture-generating mechanisms described above to naturally hydrofracture the Haynesville Shale. One well is on the Sabine Uplift which undergoes higher heat flow, less sedimentation and experienced major episodes of uplift and erosion. The other well is in the deeper part of the North Louisiana Salt Basin which has lower heat flow, greater accumulation of sediment, and less uplift and erosion.

GEOLOGIC SETTING

The northern coast of the Gulf of Mexico contains a thick sequence of predominantly shallow water Mesozoic and Cenozoic sediments (Wood and Walper, 1974; Martin, 1978; Driskill et al., 1988; Winker and Buffler, 1988; Mancini and Puckett, 2005; Galloway, 2008). Most of the onshore Mesozoic sediments are concentrated in major depositional basins in eastern Texas, northern Louisiana, and central Mississippi (Fig. 1). These depositional basins are bounded on the north and west by the continental platform and are separated by several uplifts, such as the Sabine Uplift centered on the Louisiana-Texas border and the Monroe Uplift in northeastern Louisiana (Fig. 1).

The northern Gulf Coast resulted from rifting and extension of the lithosphere during the opening of the Gulf of Mexico in the Late Triassic (Pilger, 1981; Nunn et al., 1984; Dunbar and Sawyer, 1987). Following extension, which thinned and heated the lithosphere, the region passively subsided due to conductive cooling (Nunn et al., 1984). The presence of thick Jurassic salt deposits indicates the basins formed before or during the earliest phases of opening of the Gulf.

Rifting and extension was followed by a period of cooling and subsidence of the crust and buildup of extensive carbonate platforms surrounding a deep basin in the Late Jurassic and Early Cretaceous. This was followed by a widespread mid-Cretaceous unconformity. Finally, there was progradation of a massive wedge of clastic sediments from Late Cretaceous to present (Mancini and Puckett, 2005; Galloway, 2008) (Fig. 1).

The onshore depositional basins and intervening uplifts represent short wavelength lateral variations in crustal thickness and/or composition (Nunn et al., 1984; Nunn, 1990). For example, estimates of crustal thickness from seismic refraction data are 12 mi (20 km) beneath the Central Mississippi Salt Basin and 19 mi (32 km) below the Wiggins Arch (Worzel and Watkins, 1973). There is relatively little direct information on the basement rocks underlying northern Louisiana. Most of the information is from interpretation of PASSCAL seismic data (Keller et al., 1989), gravity modeling (Mickus and Keller, 1992), and tectonic subsidence studies (Nunn et al., 1984; Dunbar and Sawyer, 1987). Based on this information, the Sabine Uplift is underlain by crust with a density similar to North American Precambrian crust and near continental thickness (22–35 mi [35–40 km]). The Sabine Uplift is separated from North America by a narrow belt of ocean-like crust overlain by Paleozoic sediments (Mickus and Keller, 1992). The most widely held interpretation is that the Sabine Uplift crust is exotic to North America perhaps representing Paleozoic arc material sutured on to North America in the late Paleozoic (Viele and Thomas, 1989). See Ewing (2009) for a recent review of the origin and tectonic/magmatic history of the Sabine Uplift.

Syn-rift uplift and erosion of the Sabine area are recognized on seismic records as a regional, low-relief unconformity (Jackson, 1982). Following uplift the region subsided and the Middle Jurassic Werner Anhydrite, Louann Salt and Norphlet clastics were deposited. Original salt thickness in the East Texas and North Louisiana salt basins is estimated at 5000 ft (1.5 km) in the central parts of the basins thinning to no more than 2000 ft (600 m) over the Sabine Uplift (Jackson and Seni, 1983; Salvador, 1987). Thin salt over the Sabine region indicates that it was a topographic high during early salt deposition, but began to disappear during the late Middle Jurassic.

During the Late Jurassic, the Sabine Uplift gradually disappeared as a separate structural unit. Jurassic Smackover Formation carbonates thin by more than 300 ft (100 m) from the center of the East Texas and North Louisiana salt basins (Anderson, 1979; McGillis, 1983). However, by the end of the Early Cretaceous, the eastern Texas–northern Louisiana region subsided as a single block and there is no significant west to east variation in either thickness or facies across the Sabine Uplift (Anderson, 1979; McGillis, 1983; Adams, 1985; Mancini et al., 2008).

Distribution of Lower Cretaceous facies and thickness variations indicate that the Sabine Uplift was at the center of a southeast-sloping basin covering all of eastern Texas and northern Louisiana (Halbouty and Halbouty, 1982; Jackson and Laubach, 1988; Adams, 2006). Lower Cretaceous units, after corrections for perturbations caused by salt movement (Lobao and Pilger, 1985), show uniform thickening in a west to east direction (Fig. 1). No evidence of a topographic feature in the Sabine Uplift area is apparent (Granata, 1963).

In the mid-Cretaceous, the Gulf of Mexico region experienced a widespread unconformity (Buffler and Sawyer, 1985). Tilting and progressive increase in age of units below the unconformity across eastern Texas and northern Louisiana indicates upwarp and subaerial exposure of the Sabine Uplift region. Estimates of the maximum erosion amounts of Late Cretaceous units range from 850 ft (260 m) (Jackson and Laubach, 1988) to 1250 ft (380 m) (Halbouty and Halbouty, 1982). Following erosion of Lower Cretaceous beds, Tuscaloosa sediments were deposited on the flanks and possibly the top of the present Sabine Uplift (Halbouty and Halbouty, 1982). Additional erosion may have occurred after deposition of the Tuscaloosa Formation. Halbouty and Halbouty (1982) estimated 300 ft (100 m) of post-Tuscaloosa erosion on the crest of the Sabine Uplift. Tuscaloosa sediments are missing over the Sabine Uplift (Granata, 1963; Halbouty and Halbouty, 1982; Jackson and Laubach, 1988) (Fig. 1).

The Sabine Uplift subsided slowly in shallow water during the Late Cretaceous and the Early Tertiary. Jackson and Laubach (1988) interpreted the absence of Eocene age sediments over the

Sabine Uplift region as evidence for a second, smaller phase of uplift and erosion. Sedimentation in both the Sabine Uplift and the North Louisiana Salt Basin ceased during the Eocene.

MODEL DESCRIPTION

Numerical modeling of the geologic history of a sedimentary basin includes simulation of sediment accumulation, burial, compaction, heating, and petroleum maturation through discrete time steps. Each time step in a model consists of a set of calculations that are used to generate input for the next time step. For example, the computed temperature at each time step during burial of a source rock is required to determine maturation. The time- and space-dependent differential transport equations needed for modeling and the numerical methods used for their solutions are beyond the scope of this paper but are documented in the literature (e.g., Zienkiewicz, 1977; Aziz and Settari, 1979).

The model used in this study was constructed and run using PetroMod® software produced by Schlumberger. The 1D version of the software used here is available for free download at software.informer.com/discovered/Petromod_1d_Free_Download. PetroMod® uses forward modeling, in which basin processes are modeled from the past to the present from an inferred starting condition (Welte et al., 1997). Basin history is divided into a sequence of depositional, non-depositional, or erosional events of specified age and duration. Input data include ages of units, present rock-unit thicknesses, and lithology of units as well as boundary conditions, such as basal heat flow and surface temperatures. In addition, type and amount of organic matter in source rocks and conversion kinetics for kerogen to petroleum are required.

In this study, formation tops information for two locations are used to estimate subsidence, temperature, maturation, and fluid pressure over time. The first well is located in Caddo Parish, Louisiana, near the border with Bossier Parish and is on the Sabine Uplift (SU well). The second well is located in Winn Parish just south of the Jackson Parish border in the deeper part of the North Louisiana Salt Basin (NLSB well). Well locations are given in Figure 1. Model input parameters for each well are listed in Tables 1 and 2.

Depth to tops was taken from Scardina (1982). In his study, subsurface data from 893 well logs were used to make structural trend surface maps. These maps were then filtered to remove the effects of local salt movement. The two points shown in Figure 1 represent points of maximum stratigraphic coverage. A complete discussion of subsurface data analysis is given in Scardina (1982). Uplift and erosion of sediments was estimated from Jackson and Laubach (1988) and Li (2006).

Lithologies or mixtures of lithologies were assigned to account for the lithofacies in each rock unit (Tables 1 and 2) based on information from Scardina (1982) and Zimmerman (1999). PetroMod® default physical and thermal rock properties, including thermal conductivities and heat capacities, were assigned to each lithology or mixture of lithologies. For example, permeability is estimated from porosity and grain size via an empirical correlation.

In this study, two Mesozoic source rocks in the North Louisiana Salt Basin are considered: The Haynesville Shale and the Smackover Formation. According to Mancini et al. (2008) and Talukdar (2008), the Haynesville Shale contains a type III kerogen with an estimated original total organic carbon (TOC) of 3% and a hydrogen index (HI) of 250 mg HC/g TOC. As part of a sensitivity study, we also consider a type II kerogen with a HI of 500 mg HC/g TOC as gas shales may contain type II kerogen or a mixture of types II and III. The underlying Smackover Formation, which is the regional source rock for most of the hydrocarbons in the North Louisiana Salt Basin (Sassen et al., 1987) is a type IIs kerogen with an estimated original TOC of 1% and a HI of 500 mg HC/g TOC (Mancini et al., 2006, 2008). Original TOC and HI were estimated using the method described in Daly

Table 1. Sabine Uplift well parameters.

Layer	Top, m	Base, m	Thickness, m	Age, Ma	Age End, Ma	PetroMod® Lithology
Cockfield	0	20	20	40	0	Shale (organic lean, sandy)
Midway	20	277	257	65.25	61.5	Shale (organic lean, silty)
U. Cret.	277	486	209	81.25	67.25	Limestone (shaly)
Austin	486	771	285	88.25	81.25	SHALEsand
Erosion			-250	99.5	94.75	
Paluxy	771	876	105	106.25	99.5	Limestone (Chalk, 40% calcite)
U. Glen Rose	876	1121	245	108.5	106.25	Limestone (Chalk, 40% calcite)
Mooringsport	1121	1350	229	112.25	108.5	Limestone (Chalk, 40% calcite)
Ferry Lake	1350	1402	52	113.25	112.25	Limestone (shaly)
Rodessa	1402	1531	129	116.5	113.25	SHALEcarb
James	1531	1659	128	118.5	116.5	LIMEshaly
Sligo	1659	1868	209	121.25	118.5	LIMEshaly
Hosston	1868	2615	747	132.5	121.25	Shale (organic lean, typical)
Cotton Valley	2615	3060	445	144.25	138.25	Shale (typical)
Haynesville	3060	3110	50	150.5	147.25	Shale (organic rich)
Smackover	3110	3805	695	159.25	150.5	Limestone (organic rich)

Table 2. North Louisiana Salt Basin well parameters.

Layer	Top, m	Base, m	Thickness, m	Age, Ma	Age End, Ma	PetroMod® Lithology
Cockfield	0	56	56	40	0	Shale (organic lean, sandy)
Cook Mtn.	56	267	212	44.5	40	Shale (organic lean, sandy)
Cane River	267	338	70	48.25	44.5	Shale (organic lean, sandy)
Wilcox	338	796	458	61.5	48.25	Sandstone (typical)
Midway	796	1007	212	65.25	61.5	Shale (organic lean, silty)
U. Cret.	1007	1230	223	81.25	67.25	Limestone (shaly)
Austin	1230	1488	258	88.25	81.25	SHALEsand
Tuscaloosa	1488	1653	165	95.25	88.25	SANDshaly
Erosion			-100	99.5	94.75	
Paluxy	1653	1811	158	106.25	99.5	Limestone (Chalk, 40% calcite)
U. Glen Rose	1811	2081	270	108.5	106.25	Limestone (Chalk, 40% calcite)
Mooringsport	2081	2363	282	112.25	108.5	Limestone (Chalk, 40% calcite)
Ferry Lake	2363	2458	94	113.25	112.25	Limestone (shaly)
Rodessa	2458	2610	152	116.5	113.25	SHALEcarb
James	2610	2774	164	118.5	116.5	LIMEshaly
Sligo	2774	2997	223	121.25	118.5	LIMEshaly
Hosston	2997	3960	963	132.5	121.25	Shale (organic lean, silty)
Cotton Valley	3960	4677	717	144.25	138.25	Shale (organic lean, silty)
Bossier	4677	5088	411	147.25	144.25	Shale (typical)
Haynesville	5088	5593	505	150.5	147.25	Shale (organic rich)
Smackover	5593	5899	306	159.25	150.5	Limestone (organic rich)

and Edman (1987). Burnham and Sweeney (1989) reaction kinetics were used to determine the generated mass of oil and gas.

Following Nunn (1984) and Nunn et al. (1984), regional water depth during deposition of each rock unit was set to zero in simulations. Paleowater depths for north Louisiana are believed to be shallow (less than 200 ft [60 m]) based on studies by Scardina (1982) and Zimmerman (1999).

Surface temperature was calculated through time using an option in PetroMod® that relates geologic age and mean surface paleotemperature based on plate tectonic reconstructions to present-day latitude. Present-day surface temperature in north Louisiana is approximately 65°F (19°C). Surface temperatures in the geologic past were warmer due to north Louisiana being closer to the equator and climate change.

PetroMod® requires present-day and paleo-heat flow to reconstruct the temperature history of basins and the thermal maturation of source-rock organic matter (Welte et al., 1997). Heat flow versus time was computed assuming rifting and extension of the lithosphere from 190 to 170 Ma. The amount of extension was estimated using a β factor of 1.25 for the SU well and a β factor of 1.5 for the NLSB well. Present-day heat flow was calibrated to be consistent with present-day temperatures. For the SU well, heat flow reached a maximum in the Middle Jurassic of 82 mW/m^2 and declined to 74 mW/m^2 today. For the NLSB well, heat flow reached a maximum of 70 mW/m^2 and declined to 48 mW/m^2 today. The smaller variation in heat flow versus time in the SU well is because of the smaller β factor. The higher present-day heat flow over the Sabine Uplift is consistent with temperature versus depth (D'Aquin and Nunn, 2010) and heat flow measurements above 80 mW/m^2 just to the west on the Texas-Louisiana border (Blackwell and Richards, 2004). The high present-day heat flow in the Sabine Uplift area is presumably due to higher radiogenic heat production in basement rocks due to thicker crust (Mickus and Keller, 1992) or different composition crust (Viele and Thomas, 1989).

MODEL RESULTS

Typical output for each depositional or erosional event in the model includes rock unit thickness after compaction, porosity, permeability, pore pressure, temperature, and thermal maturity at depth, and generated mass of petroleum.

Pore Pressure due to Compaction Disequilibrium

Figure 2 shows calculated porosity and permeability versus depth at present-day for the SU and NSLB wells. Porosity and permeability versus time were calculated by PetroMOD® and used to compute compaction as a function of effective stress (lithologic pressure minus fluid pressure). In both wells, porosity decreases significantly with depth from a surface porosity greater than 60% to less than 20% at 5000 ft (1.5 km) depth. There is some variation in porosity at a given depth with lithology (e.g., sand versus shale). Below 5000 ft (1.5 km) depth, porosity continues to decrease but more slowly, at least partially due to development of abnormal fluid pressure. Permeability also shows a

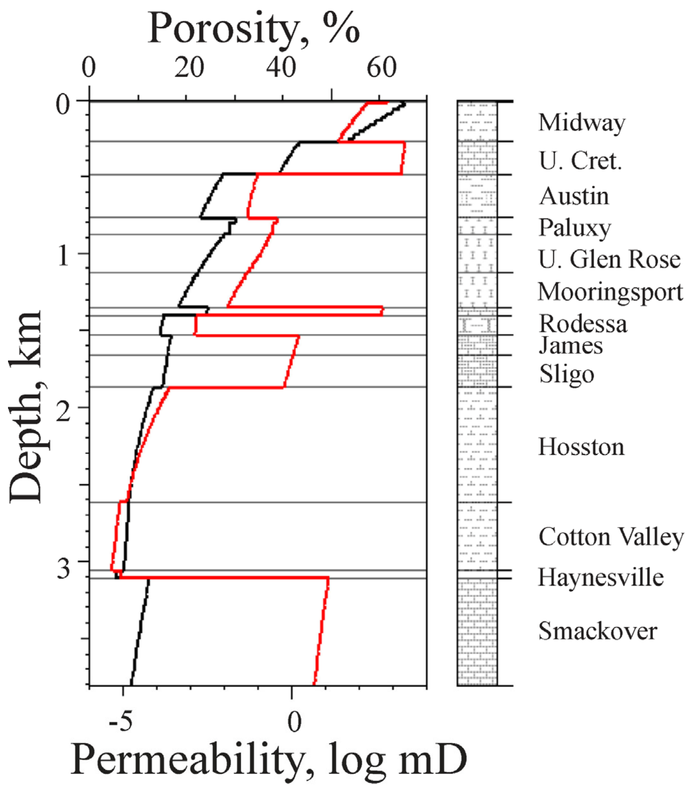

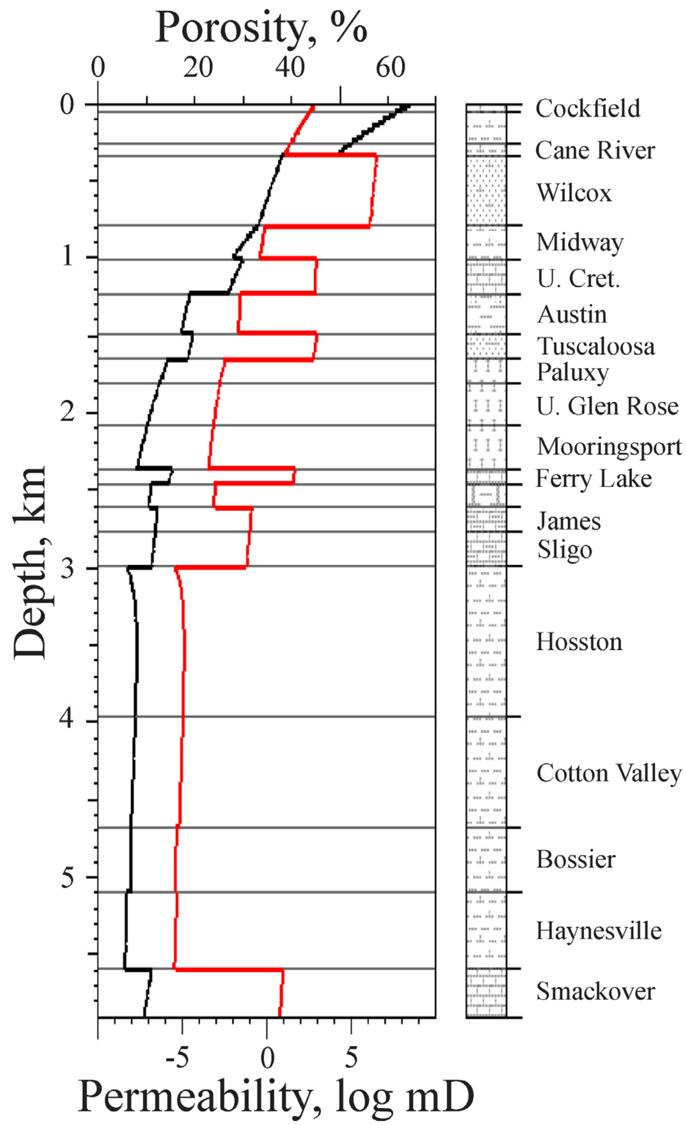

Figure 2. Present-day porosity and permeability versus depth used in modeling of thermal maturation and pressure evolution: left) Sabine Uplift well, and right) North Louisiana Salt Basin well. Black lines are porosity and red lines are permeability. See Figure 1 for well locations.

general reduction with depth although variations in permeability due to changes in lithology are much more pronounced. For example, the permeability of the Upper Cretaceous carbonates is orders of magnitude higher than the overlying shale of the Midway Formation. In the SU well, the Haynesville, Cotton Valley, and Hosston formations combine for more than a 3000 ft (1 km) thick layer of low porosity and low permeability. In the NLSB well, the Haynesville, Cotton Valley, and Hosston formations constitute a more than 8000 ft (2.5 km) thick layer of low porosity and low permeability. Present-day predicted porosity versus depth is consistent with a previous study by Talukdar (2008).

Figure 3 shows computed present-day fluid pressure versus depth due to compaction disequilibrium. During compaction, the weight of overlying sediments pushes mineral grains closer together and/or causes dissolution and precipitation of mineral grains and the pore fluid between mineral grains is forced upward (Athy, 1930). If the permeability is low enough some of the pore fluid cannot escape and thus the fluid bears some of the weight of overburden and loss of porosity is inhibited. Predicted pore pressure is plotted relative to hydrostatic pressure, lithostatic pressure and fracture pressure. Hydrostatic pressure is the pressured generated by the weight of overlying pore water. Lithostatic pressure is the weight of overlying sediment (mineral grains plus water). The fracture pressure is assumed to be 85% of the lithostatic pressure. In the SU well, predicted pore pressure is hydrostatic until a depth of 7000 ft (2.1 km) into the Hosston Formation. Predicted pore pressure exceeds hydrostatic in the thick shale of the Hosston, Cotton Valley, and Haynesville. However, overpressures are small, less than 1450 psi (10 MPa) above hydrostatic. The difference between predicted pore pressure and fracture pressure reaches a minimum in the Haynesville but is still more than 2900 psi (20 MPa). Predicted present-day pore pressure in the NLSB well is similar. Hydrostatic pressure persists to the top of the Hosston Formation at a depth of 10,000 ft (3 km). Predicted pore pressure in the Hosston, Cotton Valley, Bossier, and Haynesville exceed hydrostatic pressures by as much as 7250 psi (50 MPa) because of the greater thickness of shale, greater depth of burial, and active burial continued closer to present day (Fig. 1). While overpressures are higher in the NLSB well, the difference between predicted pore pressure and fracture pressure is still close to 2900 psi (20 MPa) in the Haynesville section.

Model results for present-day pore pressure in the Haynesville Shale are broadly consistent with observations (Wang and Hammes, 2010). Predicted overpressure of 10,750 to 11,500 psi (75–80 MPa) for the Haynesville Shale in the NLSB well are

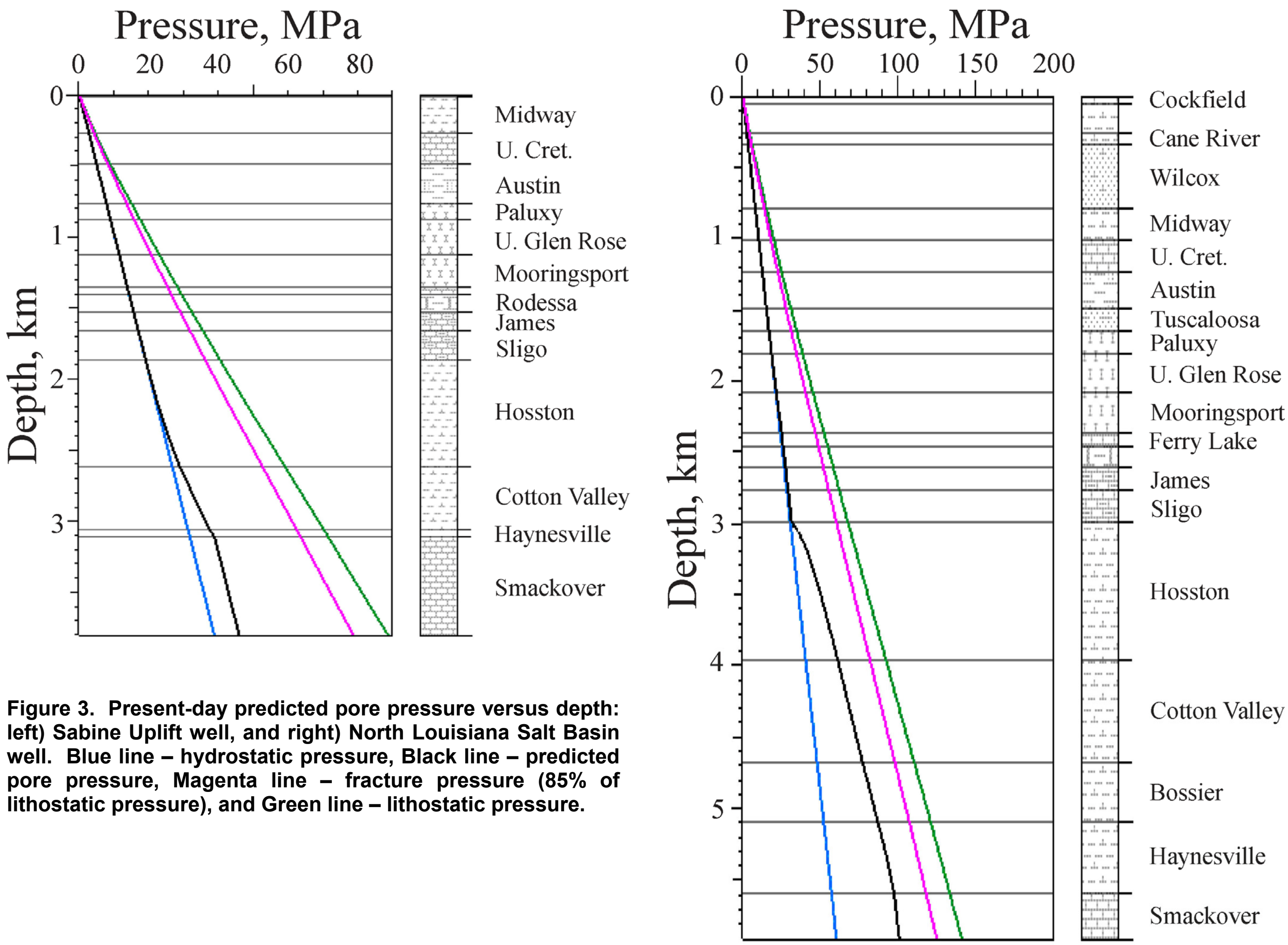

Figure 3. Present-day predicted pore pressure versus depth: left) Sabine Uplift well, and right) North Louisiana Salt Basin well. Blue line – hydrostatic pressure, Black line – predicted pore pressure, Magenta line – fracture pressure (85% of lithostatic pressure), and Green line – lithostatic pressure.

slightly higher than observed overpressures of 10,000 psi (70 MPa) in shallower sediments to the west. However, in the SU well, predicted overpressure in the Haynesville Shale of 5750 psi (40 MPa) is substantially below observed overpressures of 8000 psi (55 MPa).

Predicted pore pressure versus depth during the mid-Cretaceous for the SU well is similar to present-day (Fig. 4). There was relatively little sediment deposited in this area after the mid-Cretaceous unconformity so relatively little additional disequilibrium compaction occurred. The thick, low-permeability Hosston-Haynesville section (Fig. 2) is able to maintain overpressure for tens of millions of years (Deming, 1994). There is only a slight loss of fluid pressure at the top of the geopressured section over 100 m.y. (Figs. 3 and 4). In the NLSB well, more than 3300 ft (1 km) of additional sediment is deposited since the mid-Cretaceous unconformity. However, sedimentation rates are slower than in Jurassic-Early Cretaceous. The thick section of Hosston, Cotton Valley, Bossier, and Haynesville has predicted pore pressures well above hydrostatic. However, they are still 2150 to 2900 psi (15°20 MPa) below the fracture pressure. The primary effect of sedimentation in the NLSB over the last 100 Ma is to raise predicted fluid pressures in the upper part of the Hosston Formation. The Haynesville section remained overpressured throughout this time period with pressure gradients of 0.8 psi/ft (17.5 MPa/km) or an equivalent mud weight of 15 ppg.

Temperature and Maturity

Predicted present-day temperature versus depth for both wells is shown in Figure 5. Estimated temperatures for the Haynesville are fairly similar, 320°F (160°C) in the SU well and 355°F (180°C) in the NLSB well. There is a considerable difference in the average temperature gradient as the present-day depth of burial for the Haynesville in the SU well is just over 10,000 ft (3 km) and is more than 16,400 ft (5 km) in the NLSB well. The geothermal gradient in the NLSB well is approximately 0.0165°F/ft (30°C/km) which is consistent with an average gradient for North Louisiana estimated from Bottom Hole Temperatures (BHT) by D'Aquin and Nunn (2010). The geothermal gradient for the SU well computed from PetroMod® is 0.024°F/ft (44°C/km). This substantially higher temperature gradient is due to the higher present-day heat flow assumed for the region (Blackwell and Richards, 2004) presumably due to higher radiogenic heat production in the crust. Average geothermal gradient is the best fitting linear gradient in temperature from the surface to the base of the Smackover. Geothermal gradients vary within lithologic units due to changes in thermal conductivity even in steady state thermal conditions (Fig. 5). However, these changes in geothermal gradient are fairly small due to the small variation in thermal conductivity. Moreover, only BHTs were available for this study and usually only for one logging run per well, thus only a depth averaged geothermal gradient can be computed from observations.

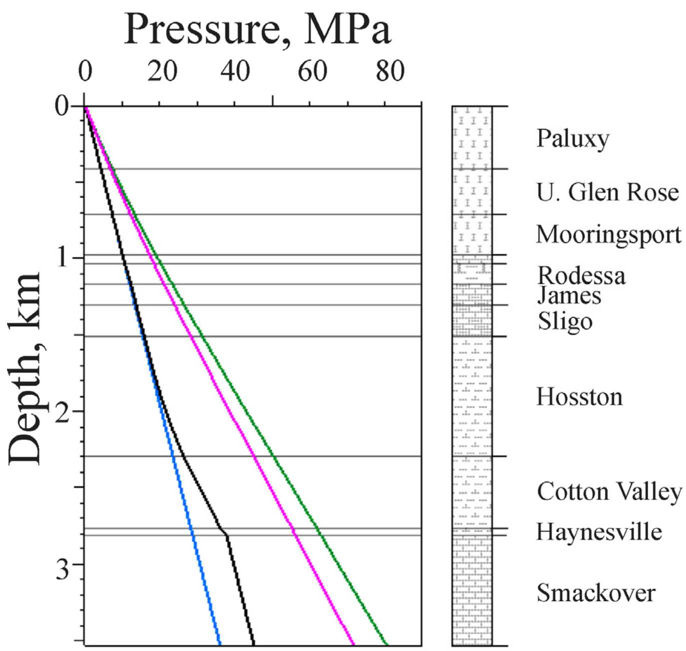

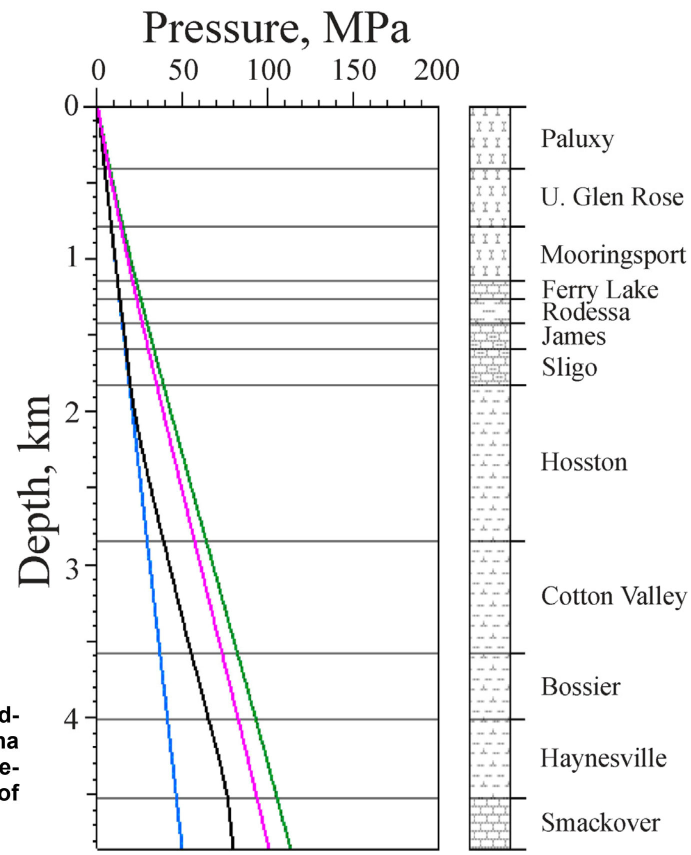

Figure 4. Predicted pore pressure versus depth in the Mid-Cretaceous: left) Sabine Uplift well, and right) North Louisiana Salt Basin well. Blue line – hydrostatic pressure, Black line – predicted pore pressure, Magenta line – fracture pressure (85% of lithostatic pressure), and Green line – lithostatic pressure.

Figure 5 also shows vitrinite reflectance (%Ro) versus depth computed from the thermal history using the EASY%Ro algorithm (Sweeney and Burnham, 1990). %Ro values for the Haynesville are 1.6 for the SU well and 1.7 for the NLSB well. Observed values of %Ro versus depth for the North Louisiana Salt Basin from Mancini et al. (2006) are shown as filled circles on Figure 5. While there is considerable scatter in the data, predicted %Ro versus depth for both wells is consistent with observations. Moreover, the SU well plots along the upper edge (higher %Ro at a given depth) and the NLSB well plots along the lower edge (lower %Ro at a given depth) of the observed values, which is consistent with model assumptions about heat flow in the two locations.

Subsidence and maturity versus time (Fig. 6) indicate that both the Smackover and Haynesville entered the oil window in the Early Cretaceous due to the combined effects of high heat flow associated with Jurassic rifting and rapid accumulation of sediment (e.g., Bossier, Cotton Valley, and Hosston). Wet gas generation begins around 100 Ma in the Smackover but maturation slows in the Late Cretaceous due to uplift and erosion. This is especially true in the SU well (Fig. 6) where wet gas generation in the Haynesville is not predicted until the Early Tertiary (60 Ma) and the Haynesville fails to reach dry gas generation (Fig. 6). In the NLSB well, the Haynesville is predicted to reach dry gas generation in the Early Tertiary (65 Ma). Additional maturation occurs in the Tertiary due to slow burial and continued warming as rapidly accumulated Early Cretaceous sediments reach thermal equilibrium. In both wells, the Smackover, Haynesville, and lower Cotton Valley are in the gas window (%Ro = 1.3), overlying Lower Cretaceous sediments (Hosston to Mooringsport) are in the oil window (%Ro = 0.55), and Upper Cretaceous and Tertiary sediments are immature. These model results are consistent with other studies (e.g., Mancini et al., 2005, 2006; Li, 2006).

Predicted temperature and maturity versus time for the Haynesville Shale are shown in Figure 7. Temperatures for the Haynesville Shale in both wells rose rapidly from 150 to 100 Ma due to rapid burial and high basal heat flow associated with rifting and extension of the lithosphere. Temperatures were near maximum values by the mid-Cretaceous. Haynesville Shale temperatures were nearly constant during the Tertiary as thermal effects of slow burial were offset by declining basal heat flow. Figure 7 also shows the impact of uplift and erosion or non-deposition on temperature. In both wells, temperature declined due to uplift and erosion in the mid-Cretaceous. The temperature decline is greater in the Sabine Uplift area because of greater erosion (800 ft [250 m] versus 330 ft [100 m]) compared to the North Louisiana Salt Basin. Declines in temperature or changes in the rate of temperature variation with time are also associated with other episodes of non-deposition or erosion (e.g., Early Cretaceous).

Model maturation versus time shows that the Haynesville Shale entered the oil window (%Ro = 0.55) in the Early Cretaceous in both locations (Fig. 7). The period of most rapid increase in organic maturity occurred between 110 and 100 Ma when rapid burial pushed model temperatures over 300°F (150° C). There was also a significant increase in the rate of organic maturation between 65 Ma and 40 Ma (Fig. 7). Model results show the Haynesville Shale entered the gas window (%Ro = 1.3) by 110 Ma in the NLSB well but not until 80 Ma in the SU well.

As noted above, model pore pressures from compaction disequilibrium do not exceed fracture pressure in either well. Another potential contribution to pore pressure is hydrocarbon generation as oil and gas have larger volumes than the kerogen

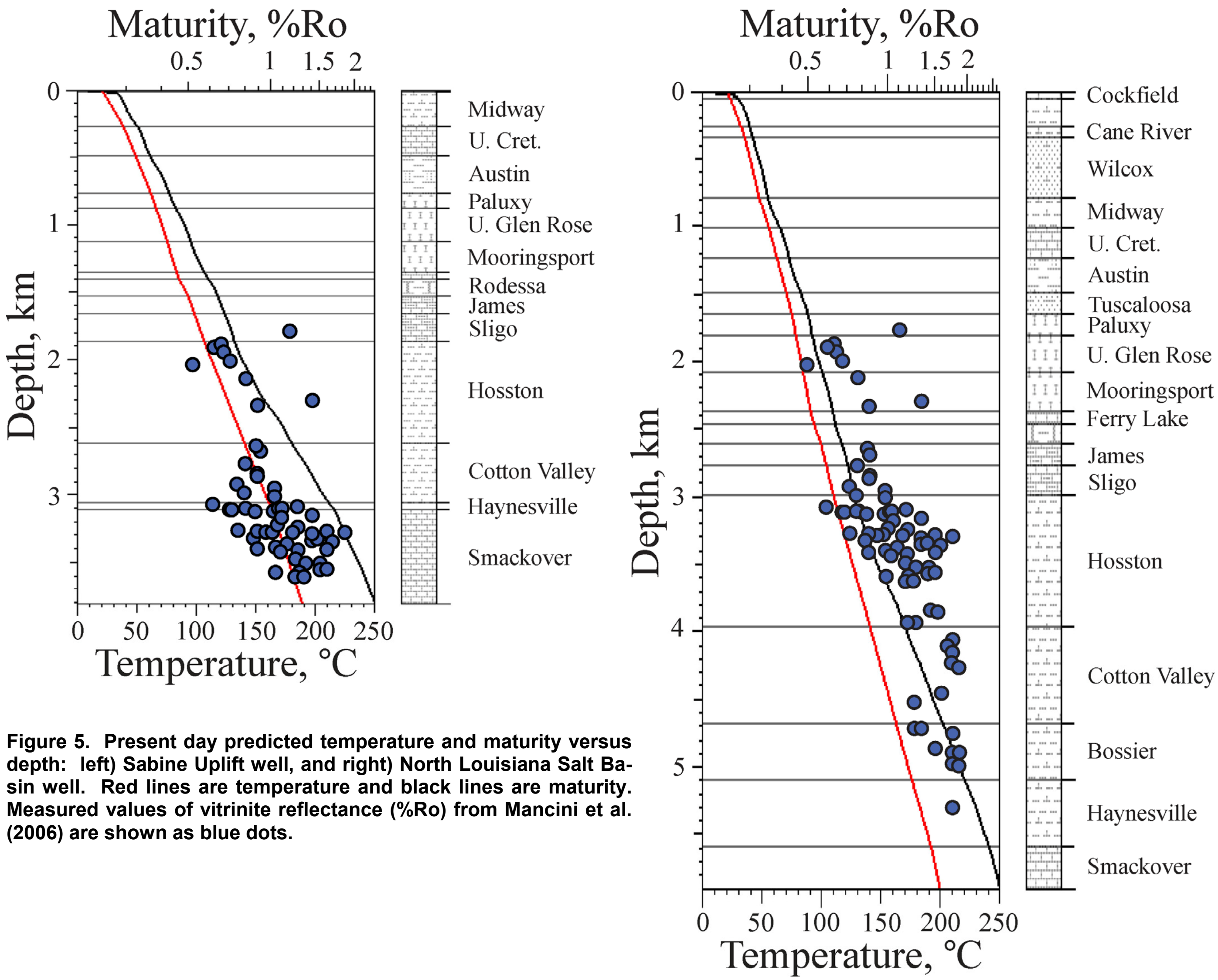

Figure 5. Present day predicted temperature and maturity versus depth: left) Sabine Uplift well, and right) North Louisiana Salt Basin well. Red lines are temperature and black lines are maturity. Measured values of vitrinite reflectance (%Ro) from Mancini et al. (2006) are shown as blue dots.

from which they form (Ungerer et al., 1983; Spencer, 1987). Figure 8 shows PetroMod® results for pressure generation due to hydrocarbon maturation versus time for the Haynesville Shale and the Smackover Formation. In both wells, there was pore pressure generation in the Smackover Formation from 140 Ma to 120 Ma. However, this pore pressure dissipated during a period of slower maturation from 120 to 110 associated with slow sediment accumulation (Figs. 7 and 8). In the NLSB well, excess pore pressure was also generated in the Haynesville Shale during this time. There was a period of pore pressure generation in the Haynesville Shale predicted for both wells in the mid-Cretaceous (110 to 95 Ma) which then dissipates due to uplift and erosion (Fig. 8). Finally, there was another wave of predicted pore pressure generation in both wells during the Tertiary (60 to 30 Ma). Unfortunately, for the default material properties used here, the magnitude of pore pressure generation by hydrocarbon generation is less than 30 psi (0.2 MPa). Thus, predicted pore pressure in the Haynesville Shale does not exceed the fracture pressure.

DISCUSSION

Model results for temperature and maturity in both wells are consistent with available information on present-day temperatures (D'Aquin and Nunn, 2010) and vitrinite reflectance (Mancini et al., 2006) as well as previous studies on thermal and maturation history of the Northern Gulf Coast interior salt basins (e.g., Nunn, 1984; Nunn and Sassen, 1986; Driskill et al., 1988; Zimmerman, 1999; Zimmerman and Sassen, 1993; Li, 2006; Mancini et al., 2008, Talukdar, 2008).

Porosity and permeability values for present-day are shown in Figure 2. Porosity values are similar to other modeling studies of the North Louisiana Salt Basin (Li, 2006; Mancini, 2008; Talukdar, 2008). Model porosity and permeability values for the Haynesville Shale are consistent with measurements from eastern Texas core samples (Wang and Hammes, 2010). Thermal conductivity for a unit varies based on porosity, mineralogy, and temperature. Thermal conductivity for model sediments varies from 1.2 to 2.5 mW/m^2 primarily due to changes in porosity which is consistent with a stratigraphic section dominated by shale and carbonate (Brigaud and Vasseur, 1989). Lithologic units with a high proportion of quartz or calcite/dolomite have higher conductivity than clay dominated units with the same porosity. Salt has a high thermal conductivity and while present in the North Louisiana Salt Basin is not included in simulations for either well.

Model results for present-day pore pressures in the Haynesville Shale are broadly consistent with observations (Wang and Hammes, 2010) even though model predictions are slightly

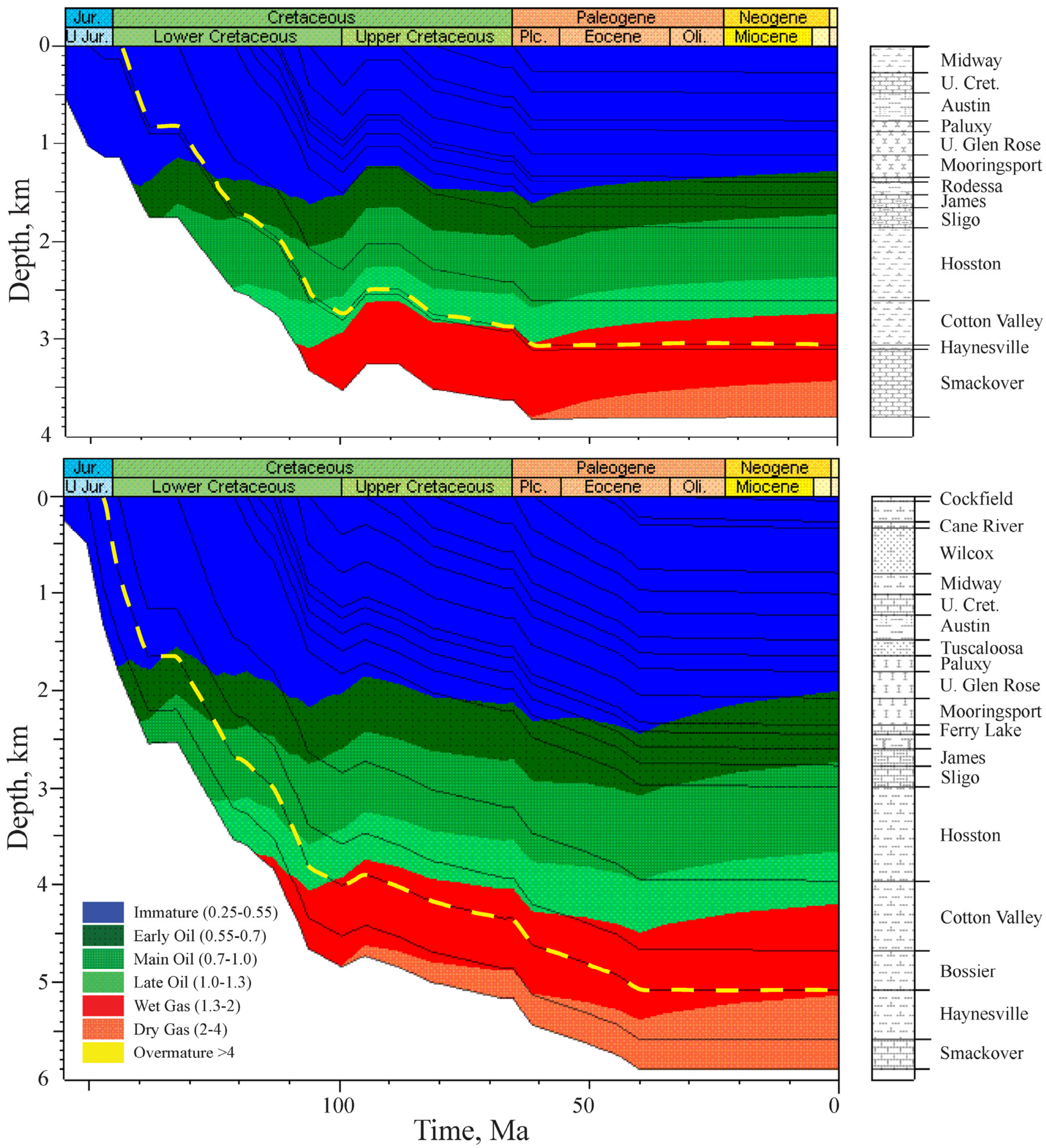

Figure 6. Predicted burial and maturation versus time: top) Sabine Uplift well, and bottom) North Louisiana Salt Basin Well. Solid lines represent burial versus time for each model stratigraphic layer. Colors indicate predicted maturation computed from the temperature history. The top of the Haynesville Shale is highlighted with a dashed yellow line.

higher than observations in the NLSB well and substantially lower than observations in the SU well. A number of factors make it difficult to explain observed overpressures of more than 8000 psi (55 MPa) in the Sabine Uplift area solely due to compaction disequilibrium, hydrocarbon generation, and only vertical transport of fluids. Total accumulation of sediments is less than 13,500 ft (4 km), uplift and erosion has removed some of the vertical load, and little sedimentation has occurred over the last 60 m.y. Thus, less overpressure is generated and loss of pore pressure over geologic time is likely (Deming, 1994).

In the present model, the Haynesville Shale is characterized as an organic rich shale. Lithology and permeability was assigned by PetroMod® based on that lithology. It is possible that all or some portions of the Haynesville Shale may have permeability values that are lower than predicted by the numerical model and thus predicted overpressure is too low. For example, Nunn (2010) conducted some simple calculations of overpressure in the Haynesville Shale using a thin 100 ft (30 m), low permeability unit which experienced rapid sedimentation followed by uplift and erosion. If the shale has a vertical permeability of 10 nd, overpressures of approximately 435 psi (3 MPa) are produced. For 1 nd permeability, overpressures of more than 1300 psi (9 MPa) are generated. In both instances, the pore pressure pulse dissipated on time scales of 10 m.y. because the shale is thin (Deming, 1994). However, a short pulse of high pore pressure could hydrofracture the shale. Matrix permeability for the

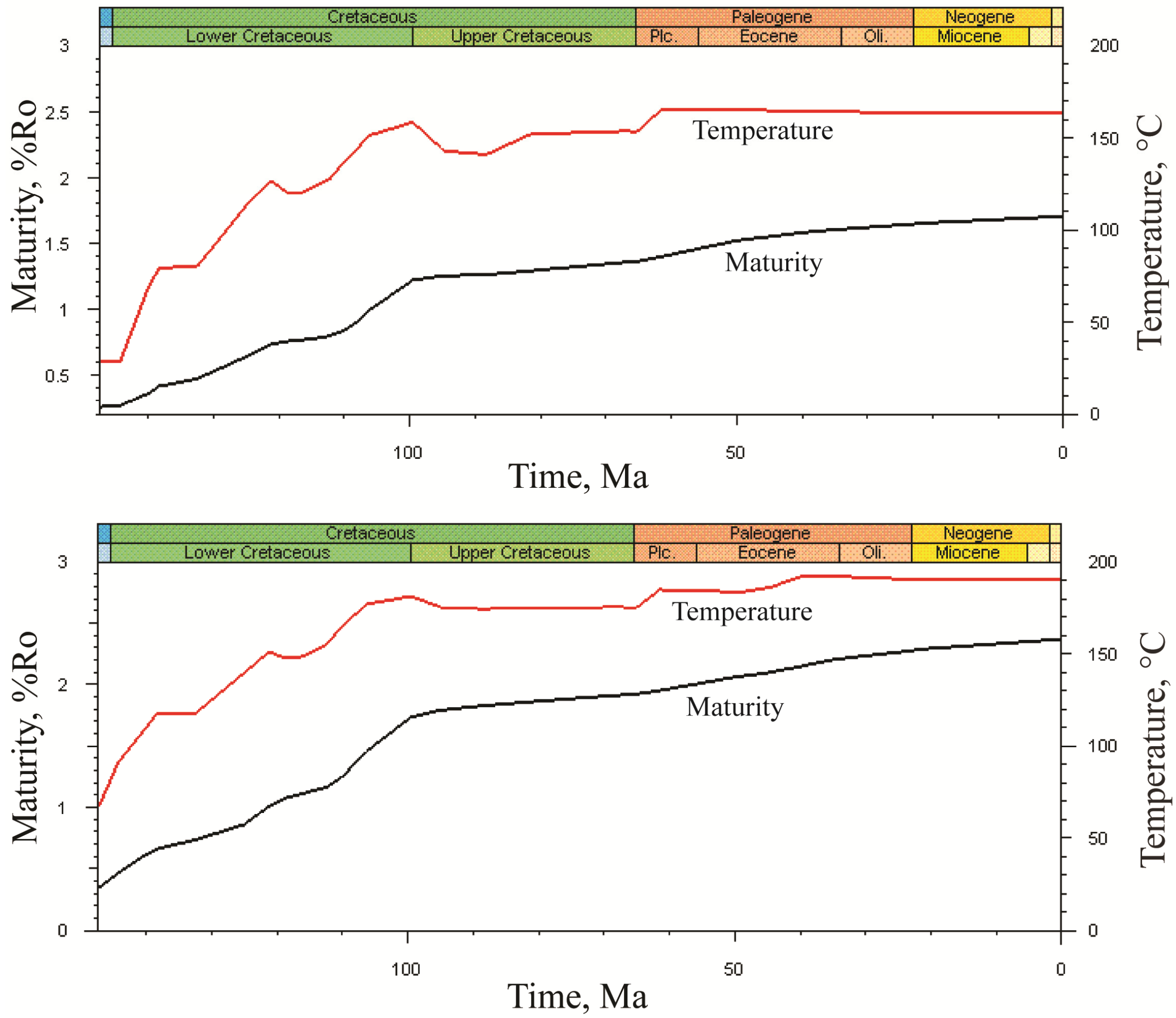

Figure 7. Predicted temperature and maturation history for the Haynesville Shale: top) Sabine Uplift well, and bottom) North Louisiana Salt Basin well. Red lines are temperature and black lines are maturity.

Haynesville Shale in eastern Texas measured from crushed core samples varies by orders of magnitudes and is as low as 0.01 nd (Wang and Hammes, 2010). Pore pressure required to hydrofracture sediment also depends on elastic properties (Hubbert and Willis, 1957) which could also vary in space and time. Thus, natural hydrofractures could be a localized phenomena.

It is important to note that generating pore pressures near fracture pressures for the burial/temperature history of the Haynesville Shale assuming only 1D disequilibrium compaction requires low permeability at shallow depth. For example, 1D simulations using a uniform shale lithology do not reach fracture pressures. Some sort of low permeability seal, such as anhydrite, is required (W. Torsch, 2012, personal communication).

It is also possible that for ultralow permeability units, such as organic-rich shales, other pressure- generating processes may be important such as aquathermal pressuring (Barker, 1972; Sharp, 1983) or smectite to illite transformation (Freed and Peacor, 1989), as well as hydrocarbon generation.

Different choices for hydrocarbon parameters such as original TOC, kerogen type, or hydrocarbon index may also influence model results. For example, Talukdar (2008) ran simulations of the Haynesville Shale for type III kerogen with HI of 200 mg HC/g TOC and a combination of Types II and III kerogen with a HI of 350 mg HC/g TOC. The later set of parameters generated almost twice as much oil and gas and thus would generate higher overpressures. Figure 9 compares generation mass for the a type III kerogen with a HI of 200 mg HC/g TOC with a type II kerogen with a HI of 500 mg HC/g TOC. Type II kerogen generates more than twice as much hydrocarbon and most of it is oil. Thus, type II generates additional pore pressure. If TOC is increased to 10% and permeability is decreased by an order of magnitude, then predicted pressure generation is 300–450 psi (2–3 MPa). Oil and gas generation for type II kerogen also occurs earlier which means that pressure generation occurs primarily in the Early Cretaceous and the pore pressure generation in the Tertiary is smaller because of less gas generation late in the basin history.

The low pressure generation in the Haynesville Shale associated with hydrocarbon maturation was surprising. While it was expected that this effect would be smaller than disequilibrium compaction it was anticipated to be smaller by a factor of 2–3 (Hanson and Lee, 2005) rather than one or more orders of magnitude. There are several reasons why hydrocarbon generation is small in our simulations. As previously noted, the Haynesville Shale is a thin unit (~100 m), thus overpressure bleeds off to adjacent units (Deming, 1994) especially the higher porosity and permeability Smackover formation (Fig. 2). In the original simulations, a type III (gas prone) kerogen is used. Methane is highly compressible so that under in situ conditions the vapor density is

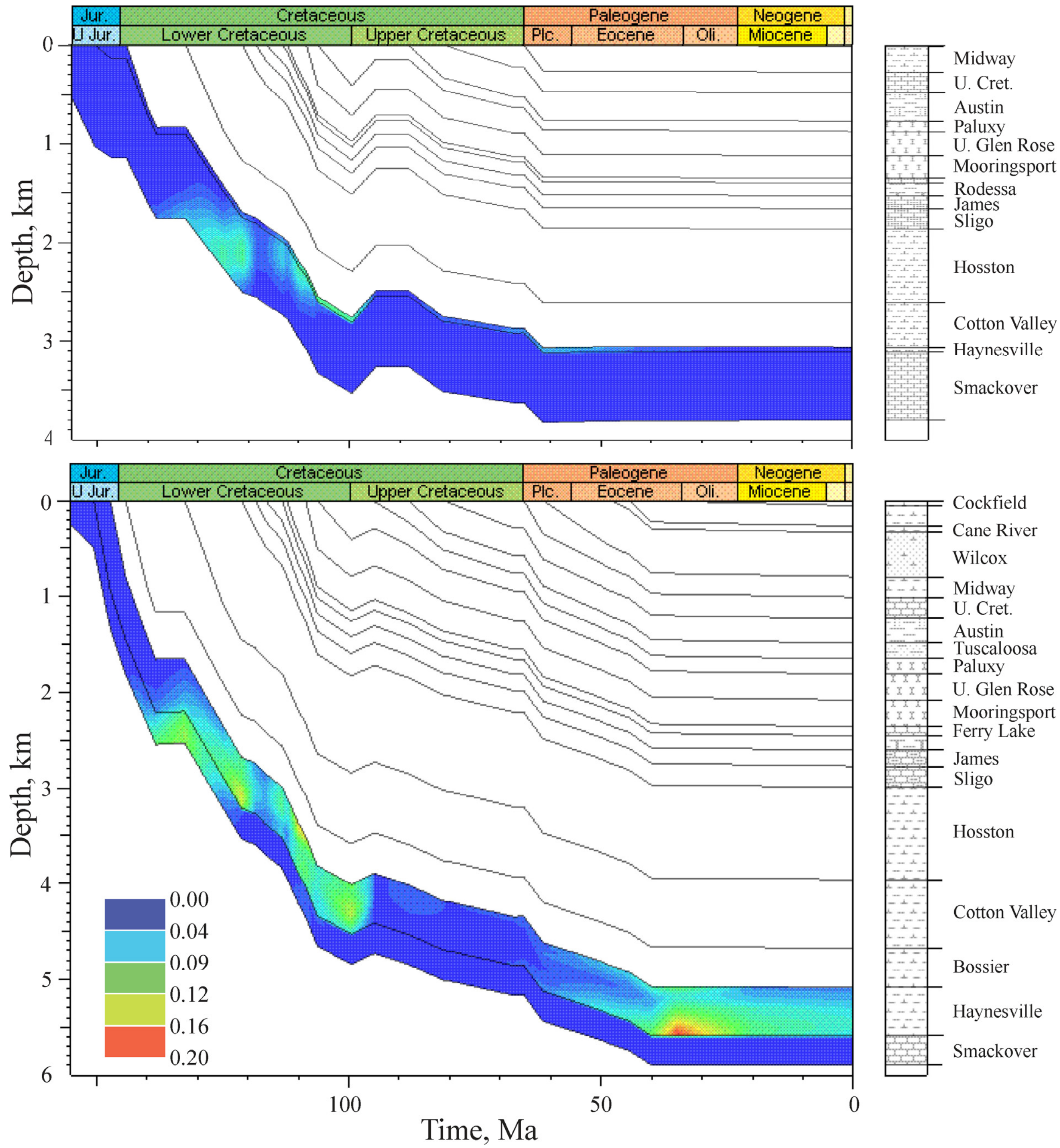

Figure 8. Predicted pressure generation by hydrocarbon maturation during burial in Haynesville and Smackover units. top) Sabine Uplift well, and bottom) North Louisiana Salt Basin well. See text for explanation.

between 300–500 Kg/m3 so the impact on pore pressure is limited. A TOC of 3% is assumed whereas porosity is approximately 10% due to undercompaction so volumetrically there is little methane spread thorough a still substantial pore space. Numerical simulations of pressure generation in Eugene Island, offshore Louisiana using the Platte River Associates BasinMod 2–D also predict a small amount of overpressure (300–450 psi [2–3 MPa]) due to hydrocarbon generation (Ajit Joshi, 2011, personal communication).

Recent studies (Mango and Jarvie, 2009) suggest that reaction rates for gas generation at low temperatures may be faster in marine shale than in other lithologies. This would likely decrease maximum overpressure predictions as hydrocarbon generation would occur at shallow burial depths before compaction disequilibrium is fully developed.

Low predicted pressure generation by thermal maturation of hydrocarbons also may be due to numerical limitation. In most numerical schemes, changes propagate one numerical node each time step. The node spacing of 10 m and time step of 1 million years used in this study may be too coarse to adequately capture pressure generation within the thin Haynesville Shale (~100 m). This is the subject of an ongoing study.

Conservative erosion amounts of 330 ft (100 m) and 825 ft (250 m) for the NLSB and SU wells, respectively, were used in the model simulations. Erosion may have been greater (Halbouty and Halbouty, 1982). Simulations for the SU well in which uplift

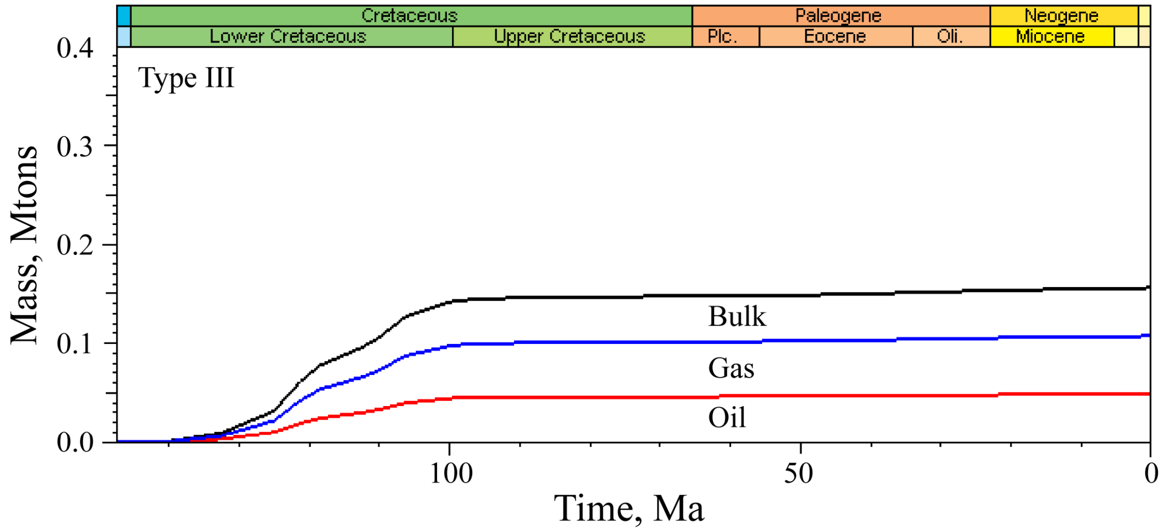

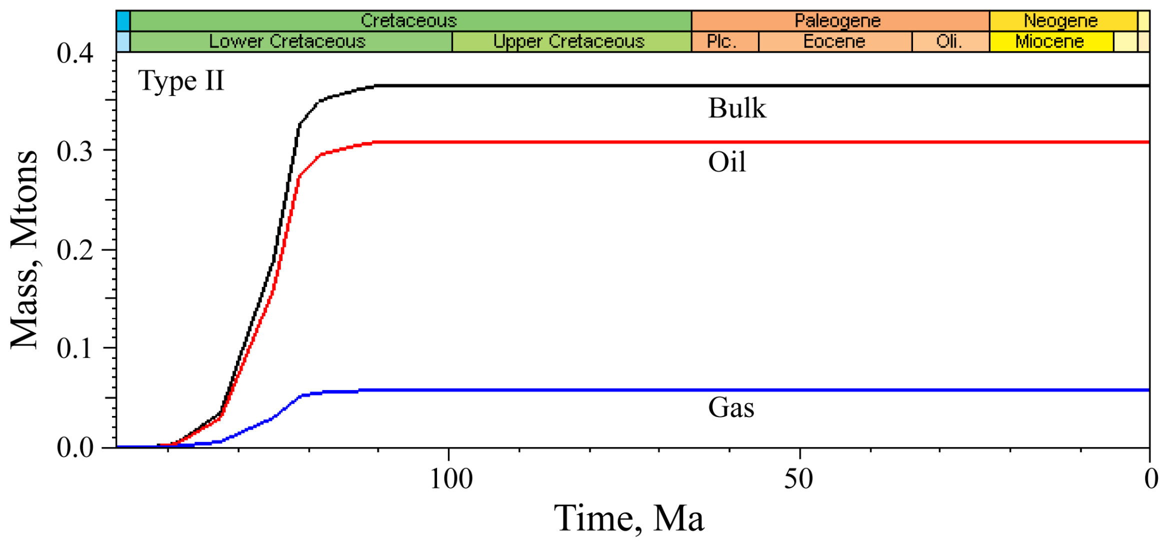

Figure 9. Predicted mass of hydrocarbons generated versus time in the Haynesville Shale for the North Louisiana Salt Basin well: top) Type III kerogen with a HI index of 250 mg HC/g TOC, and bottom) Type II kerogen with a HI index of 500 mg HC/g TOC. Red line is oil, blue line is gas, and black line is bulk (oil plus gas).

and erosion was varied from 330 to 1325 ft (100 to 400 m) showed little difference. Results for present-day temperature, maturation and pore pressure are identical. In simulations with more erosion, higher temperatures and pore pressures are predicted immediately prior to erosion because of more sedimentation. Subsequently, the model predicts a larger drop in temperature and pore pressure during erosion. Within a few million years after the end of erosion all simulations have the same maturation levels/pore pressures for the Haynesville Shale. Thus, the primary effect of more uplift and erosion in simulations is to have a pulse of additional maturation (up to 0.1 %Ro) and pore pressure immediately prior to erosion. As the models predict that the Haynesville Shale is near the gas window at this time a maximum erosion simulation case would have gas generation 10–15 m.y. earlier than a minimum erosion case.

In this study, the primary effect of uplift and erosion is to dissipate overpressure (Fig. 8) which makes natural hydrofractures less likely. Material properties used in this study are default parameters for specified lithologies in PetroMod®. Different choices for permeability and compressibility of sediments could result in retention of overpressures during uplift and erosion which could potentially exceed the fracture pressure as lithostatic pressure was reduced. This is the subject of ongoing work.

Finally, the present models are one-dimensional and assume that vertical processes (sedimentation, erosion, and fluid expulsion) dominate pore pressure generation. For a permeable reservoir (~100 md or higher), it is often necessary to do a 3D simulation of pore pressure generation in order to accurately reproduced observed pore pressures. This is because lateral transport of fluid driven by spatial variations in pore pressure is significant. Sufficient information to construct a 3D model (e.g., 2D or 3D seismic data or information from scores of wells) was not available to this study. Moreover, the initial presumption was that the Haynesville Shale has very low permeability (~ nd) and thus lateral transport of fluid is limited even if large spatial variations in pore pressure exist. As a preliminary study, it was of interest to test the hypothesis that pore pressure generation due solely to vertical disequilibrium compaction and/or hydrocarbon generation could reach fracture pressures and reproduce observed present day formation pressures.

Lateral transfer of fluid pressure has been documented in the modern day Gulf of Mexico and elsewhere (Gordon and Flemings, 1998; Dugan and Flemings, 2000). In addition, other workers have proposed that gas found in reservoirs in the Monroe Uplift have migrated laterally from deeply buried Smackover source rocks in the center of the North Louisiana Salt Basin (Zimmerman and Sassen, 1993; Mancini et al., 2008). Lateral pressure transfer within the North Louisiana Salt Basin could potentially explain why the 1D models described here over predict fluid pressure in the deep part of the basin and under predict fluid pressure on the Sabine Uplift. Lateral pressure transfer would also facilitate natural hydrofracture as high fluid pressures in the interior are transmitted updip to shallower regions where lithostatic pressure is lower. This would be especially true during times of uplift and erosion. Pore pressure simulations of the Haynesville Shale in multiple dimensions including the effects of lateral pressure transfer are part of an ongoing study.

SUMMARY AND CONCLUSIONS

Rapid sedimentation in the Early Cretaceous strongly contributed to generation of overpressure by compaction disequilibrium in the Haynesville Shale and other deeply buried units. Predicted overpressures of 10,750–11,500 psi (75–80 MPa) for the Haynesville Shale in the NLSB well are roughly consistent with observed overpressures of greater than 10,000 psi (70 MPa) in shallower sediments to the west. In the SU well predicted overpressure of 5750 psi (40 MPa) in the Haynesville Shale is substantially below observed overpressures of greater than 8000 psi (55 MPa). In both wells, predicted overpressures never exceed the fracture gradient solely due to 1D compaction disequilibrium.

High heat flow in the Early Cretaceous associated with rifting of the lithosphere during the Jurassic contributed to high temperature gradients and early maturation of deep units such as the Smackover Formation and Haynesville Shale. Thus, peak hydrocarbon generation was roughly synchronous with maximum sedimentation rates in the Early Cretaceous. Hydrocarbon generation produced additional overpressure in the Late to mid-Cretaceous and the Late Paleogene. However, additional overpressure generation is small (< 300 psi [2 MPa]) and thus predicted overpressure does not exceed the fracture pressure.

Using default parameters for organic rich shale in PetroMod® software, uplift and erosion and/or non-depositional events tend to dissipate overpressure. Thus, they do not appear to contribute to natural hydrofracture. However, model results are highly sensitive to permeability and compressibility of sediments which can vary by orders of magnitude.

For ultralow permeability (nanodarcy) units such as the Haynesville, other pore pressure generating processes such as aquathermal pressuring and clay diagenesis may be important.

Lateral pressure transfer, which could explain under prediction of overpressure in the Sabine Uplift well and over prediction of overpressure in the North Louisiana Salt Basin well, should be considered in future modeling efforts.

ACKNOWLEDGMENTS

Will Torsch and Austin Cardneaux provided useful discussions on modeling pore pressure formation in shales. Detailed and constructive reviews by Mary Barrett, Brandon Dugan, Barry Katz, and Peng Li greatly improved the clarity and quality of this manuscript.

REFERENCES CITED

Adams, G. S., 1985, Depositional history and diagenesis of the middle Glen Rose Reef complex (Lower Cretaceous), East Texas and Louisiana: M.S. Thesis, Louisiana State University, Baton Rouge, 200 p.

Adams, R. L., 2006, Basement tectonics and origin of the Sabine uplift, *in* R. Turner, ed., The Gulf Coast Mesozoic sandstone gas province symposium volume: East Texas Geological Society 2006 Symposium, Tyler, Texas, p. 1–31.

Anderson, E. G., 1979, Basic Mesozoic study in Louisiana, the northern coastal region and the Gulf basin province: Louisiana Geological Survey Folio Series, v. 3, Baton Rouge, 58 p.

Athy, L., 1930, Density, porosity, and compaction of sedimentary rocks: American Association of Petroleum Geologists Bulletin, v. 14, p. 1–24.

Aziz, K., and A. Settari, 1979, Petroleum reservoir simulation: Applied Science Publishers, London, U.K., 476 p.

Barker, C., 1972, Aquathermal pressuring—Role of temperature in development of abnormal-pressure zones: American Association of Petroleum Geologists Bulletin, v. 56, p. 2068–2071.

Berg, R., J. Fulco, and D. Buller, 2009, Core presentation as part of a symposium on "Haynesville and other shale plays": Gulf Coast Association of Geological Societies Annual Meeting, Shreveport, Louisiana.

Brigaud, F., and G. Vasseur, 1989, Mineralogy, porosity and fluid control on thermal conductivity of sedimentary rocks: Geophysical Journal, v. 98, p. 525–542.

Blackwell D. D., and M. C. Richards, 2004, Geothermal map of North America: Southern Methodist University Geothermal Laboratory, <http://smu.edu/geothermal/2004NAMap/Geothermal_MapNA_7x10in.gif> Accessed September 9, 2012.

Buffler, R. T., and D. S. Sawyer, 1985, Distribution of crust and early history, Gulf of Mexico Basin: Gulf Coast Association of Geological Societies Transactions, v. 35, p. 333–344.

Burnham, A. K., and J. J. Sweeney, 1989, A chemical kinetic model of vitrinite maturation and reflectance: *Geochimcia et Cosmochimica Acta*, v. 53, p. 2649–2657.

Buller, D., and M. C. Dix, 2009, Petrophysical evaluation of the Haynesville shale in northwest Louisiana and northeast Texas: Gulf Coast Association of Geological Societies Transactions, v. 59, p. 127–143.

Daly, A. R., and J. D. Edman, 1987, Loss of organic carbon from source rocks during thermal maturation: American Association of Petroleum Geologists Bulletin, v. 71, p. 546.

D'Aquin, A., and J. A. Nunn, 2010, Enhanced geothermal potential of south Bossier parish, Louisiana: Gulf Coast Association of Geological Societies Transactions, v. 60, p. 785.

Deming, D., 1994, Factors necessary to define a pressure seal: American Association of Petroleum Geologists Bulletin, v. 78, p. 1005–1009.

Driskill, B. W., J. A. Nunn, R. Sassen, and R. H. Pilger, Jr., 1988, Tectonic subsidence, crustal thinning and petroleum generation in the Jurassic trend of Mississippi, Alabama and Florida: Gulf Coast Association of Geological Societies Transactions, v. 38, p. 257–265.

Dugan, B., and P. B. Flemings, 2000, Overpressure and fluid flow in the New Jersey continental slope: Implications for slope failure and cold seeps: Science, v. 289, p. 288–291.

Dunbar, J. A., and D. S. Sawyer, 1987, Implications of continental crust extension for plate reconstruction: An example from the Gulf of Mexico: Tectonics, v. 6, p. 739–755.

Ewing, T. E., 2009, The ups and downs of the Sabine Uplift and the northern Gulf of Mexico Basin: Jurassic basement blocks, Cretaceous thermal uplifts, and Cenozoic flexure: Gulf Coast Association of Geological Societies Transactions, v. 59, p. 253–269.

Fan, L., J. W. Thompson, and J. R. Robinson, 2010, Understanding gas production mechanism and effectiveness of well stimulation in the Haynesville shale through reservoir simulation: Canadian Society for Unconventional Gas (Calgary, Alberta) / Society of Petroleum Engineers (Richardson, Texas) Paper 136696.

Freed, R. L, and D. R. Peacor, 1989, Geopressured shale and sealing effect of smectite to illite transition: American Association of Petroleum Geologists Bulletin, v. 73, p. 1223–1232.

Galloway, W. E., 2008, Depositional evolution of the Gulf of Mexico sedimentary basin, *in* A. D. Miall, ed., Sedimentary basins of the world, v. 5: The sedimentary basins of the United States and Canada: Elsevier, Amsterdam, The Netherlands, p. 505–549.

Gordon, D. S., and P. B. Flemings, 1998, Generation of overpressure and compaction-driven fluid flow in a Plio-Pleistocene growth-faulted basin, Eugene Island 330, offshore Louisiana: Basin Research, v. 10, p. 177–196.

Granata, W. H., Jr., 1963, Cretaceous stratigraphy and structural development of the Sabine Uplift area, Texas and Louisiana, *in* Report on selected North Louisiana and South Arkansas oil and gas fields: Shreveport Geological Society Reference Report, v. 5, p. 50–95.

Halbouty, M. T., and J. J. Halbouty, 1982, Relationships between East Texas Field region and Sabine Uplift in Texas: American Association of Petroleum Geologists Bulletin, v. 66, p. 1042–1054.

Hansom, J., and M.-K. Lee, 2005, Effects of hydrocarbon generation, basal heat flow and sediment compaction on overpressure development: A numerical study: Petroleum Geoscience, v. 11, p. 353–360.

Hubbert, M. K., and D. G. Willis, 1957, Mechanics of hydraulic fracturing: Journal Petroleum Technology, v. 9, p. 153–166.

Jackson, M. P. A., 1982, Fault tectonics of the East Texas Basin: Texas Bureau of Economic Geology Geological Circular 82–4, Austin, 31 p.

Jackson, M. L. W., and S. E. Laubach, 1988, Cretaceous and Tertiary compressive tectonics as the cause of the Sabine Arch, East Texas and Northeast Louisiana: Gulf Coast Association of Geological Societies Transactions, v. 38, p. 245–256.

Jackson, M. P. A., and S. J. Seni, 1983, Geometry and evolution of salt structures in a marginal rift basin of the Gulf of Mexico, East Texas: Geology, v. 11, p. 131–135.

Keller, G. R., L. W. Braile, G. A. McMechan, W. A. Thomas, S. H. Harder, W.-F. Chang, and W. G. Jardine, 1989, Paleozoic continent-ocean transition in the Ouachita mountains imaged from PASSCAL wide-angle seismic reflection-refraction data: Geology, v. 17, p. 119–122.

Li, P., 2006, Modeling of thermal maturity history of strata in the North Louisiana Salt Basin area: Gulf Coast Association of Geological Societies Transactions, v. 56, p. 439–454.

Lobao, J. J., and R. H. Pilger Jr., 1985, Early evolution of salt structures in the North Louisiana Salt Basin: Gulf Coast Association Geological Societies Transactions, v. 35, p. 189–198.

Mancini, E. A., and T. M. Puckett, 2005, Jurassic and Cretaceous transgressive-regressive (T-R) cycles, northern Gulf of Mexico, U.S.A.: Stratigraphy, v. 2, p. 31–48.

Mancini, E. A., P. Li, D. A. Goddard, and R. K. Zimmerman, 2005, Petroleum source rocks of the onshore interior salt basins, north central and northeastern Gulf of Mexico: Gulf Coast Association of Geological Societies Transactions, v. 55, p. 486–504.

Mancini, E. A., D. A. Goddard, R. Barnaby, and P. Aharon, 2006, Basin analysis and petroleum system characterization and modeling, interior salt basins, central and eastern Gulf of Mexico: U.S. Department of Energy Final Technical Report, Phase 1, Project Number DE–FC26–03NT15395, 422 p.

Mancini, E. A., P. Li, D. A. Goddard, V. Ramirez, and S. C. Talukdar, 2008, Mesozoic (Upper Jurassic–Lower Cretaceous) deep gas reservoir play, central and eastern Gulf Coastal Plain: American Association of Petroleum Geologists Bulletin, v. 92, p. 283–208.

Mango, F. D., and D. M. Jarvie, 2009, Low-temperature gas from marine shales: Geochemical Transactions, v. 10, 8 p.

Martin, R. G., 1978, Northern and eastern Gulf of Mexico continental margin: Stratigraphic and structural framework: American Association of Petroleum Geologists Studies in Geology 7, Tulsa, Oklahoma, p. 21–42.

McGillis, K. A., 1983, Stratigraphy and diagenesis of the Upper Jurassic, northeast Texas: M.S. Thesis, Louisiana State University, Baton Rouge, 154 p.

Mello, U. T., and G. D. Karner, 1996, Development of sediment overpressure and its effect on thermal maturation: Application to the Gulf of Mexico Basin: American Association of Petroleum Geologists Bulletin, v. 80, p. 1367–1396.

Mickus, K. L., and G. R. Keller, 1992, Lithospheric structure of the south-central United States: Geology, v. 20, p. 335–338.

Nunn, J. A., 1984, Subsidence histories for the Jurassic sediments of the northern Gulf Coast: Thermal-mechanical model, *in* W. P. S. Ventress, D. G. Bebout, B. F. Perkins, and C. H. Moore, eds., The Jurassic of the Gulf rim: Proceedings of the 3rd Annual Gulf Coast Section of the Society of Economic Mineralogists and Paleontologists Foundation Research Conference, Houston, Texas, p. 309–322.

Nunn, J. A., 1990, Relaxation of continental lithosphere: An explanation for Late Cretaceous reactivation of the Sabine Uplift of Louisiana-Texas: Tectonics, v. 3, p. 341–359.

Nunn, J. A., 2010, Uplift, subsidence, and reactivation of the Sabine Uplift due to changes in flexural compensation between different crustal blocks: Implications for the burial and thermal history of the Haynesville shale, <http://www.searchanddiscovery.com/abstracts/pdf/2010/annual/abstracts/ndx_nunn.pdf> Last Accessed September 9, 2012.

Nunn, J. A., A. D. Scardina, and R. H., Pilger, Jr, 1984, Thermal evolution of the north-central Gulf Coast: Tectonics, v. 3, p. 723–740.

Nunn, J. A., and R. Sassen, 1986, The framework of hydrocarbon generation and migration, Gulf of Mexico continental slope: Gulf Coast Association of Geological Societies Transactions, v. 36, p. 257–262.

Osborne, M. J., and R. E. Swarbrick, 1997, Mechanisms for generating overpressure in sedimentary basins: A reevaluation: American Association of Petroleum Geologists Bulletin, v. 81, p. 1023–1041.

Pilger, R. H., Jr., 1981, The opening of the Gulf of Mexico: Implications for the tectonic evolution of the northern Gulf Coast: Gulf Coast Association of Geological Societies Transactions, v. 31, p. 377–381.

Salvador, A., 1987, Late Triassic – Jurassic paleogeography and origin of Gulf of Mexico Basin: American Association of Petroleum Geologists Bulletin, v. 71, p. 419–451.

Sassen, R., C. H. Moore, and F. C. Meendsen, 1987, Distribution of hydrocarbon source potential in the Jurassic Smackover Formation: Organic Geochemistry, v. 11, p. 379 –383.

Scardina, A. D., 1982, Tectonic subsidence history of the North Louisiana Salt Basin: Louisiana State University Publications in Geology and Geophysics, Gulf Coast Studies, Baton Rouge, v. 2, 34 p.

Sharp, J. M., Jr., 1983, Permeability controls on aquathermal pressuring: American Association of Petroleum Geologists Bulletin, v. 67, p. 2057–2061.

Spencer, C. W., 1987, Hydrocarbon generation as a mechanism for overpressuring in Rocky Mountain region: American Association of Petroleum Geologists Bulletin, v. 71, p. 368–388.

Sweeney, J. J., and A. K. Burnham, 1990, Evaluation of a simple model of vitrinite reflectance based on chemical kinetics:

American Association of Petroleum Geologists Bulletin, v. 74, p. 1559–1570.

Talukdar, S. C., 2008, Application of geochemistry for shale gas assessment, <http://www.fwgs.orgcTalukdarASSESSMENT.pdf> Last Accessed September 9, 2012.

Ungerer, P., E. Behar, and D. Discamps, 1983, Tentative calculation of the overall volume expansion of organic matter during hydrocarbon genesis from geochemistry data. Implications for primary migration, *in* M. Bjoroy, ed., Advances in organic geochemistry: Wiley, New York, New York, p. 129–135.

Viele, G. W., and W. A. Thomas, 1989, Tectonic synthesis of the Ouachita orogenic belt, *in* R. D. Hatcher, Jr., W. A. Thomas, and G.W. Viele, eds., The geology of North America, v. F–2: The Appalachian-Ouachita orogen in the United States: Geological Society of America, Boulder, Colorado, p. 695–728.

Wang, F. P., and U. Hammes, 2010, Effects of petrophysical factors on Haynesville fluid flow and production: World Oil, v. 231, p. D79–D82.

Welte, D. H., B. Horsfield, and D. R. Baker, eds., 1997, Petroleum and basin evolution: Springer-Verlag, New York, 535 p.

Winker, C. D., and R. T. Buffler, 1988, Paleogeographic evolution of early deep-water Gulf of Mexico and margins, Jurassic to middle Cretaceous (Cenomanian): American Association of Petroleum Geologists Bulletin, v. 72, p. 318–346.

Wood, M. L., and J. L. Walper, 1974, The evolution of the interior Mesozoic basin and the Gulf of Mexico: Gulf Coast Association of Geological Societies Transactions, v. 24, p. 31–41.

Worzel, J. L., and J. S. Watkins, 1973, Evolution of the northern Gulf Coast deduced from geophysical data: Gulf Coast Association of Geological Societies Transactions, v. 23, p. 84–91.

Zienkiewicz, O. C., 1977, The finite element method: McGraw-Hill, London, U.K., 787 p.

Zimmerman, R. K., 1999, Potential oil generation capacity of the north Louisiana hydrocarbon system: Gulf Coast Association of Geological Societies Transactions, v. 49, p. 532–540.

Zimmerman, R. K., and R. Sassen, 1993, Hydrocarbon transfer pathways from Smackover source rocks to younger reservoir traps in the Monroe Gas Field, northeast Louisiana: Gulf Coast Association of Geological Societies Transactions, v. 43, p. 473–480.